Calcium-induced inactivation of NMDA receptor–channels evolves independently of run-down in cultured rat brain neurones

Igor Medina, Natalia Filippova, Akhmatgan Bakhramov and Piotr Bregestovski*

INSERM, Unité 29, Hôpital de Port-Royal, 123 boulevard de Port-Royal, 75014 Paris, France

1. Calcium-induced transient inactivation of NMDA receptor (NMDAR) channels was studied in cultured rat hippocampal and cerebellar granule neurones using patch-clamp techniques and confocal scanning microscopy.

2. During whole-cell recordings, in the presence of 2 mM external Ca^{2+}, conditioning (2–20 s) pulses of NMDA (20–100 μM) caused a transient decrease in NMDA responses. Recovery developed in two phases with time constants of 0·6 and 40 s. The slow phase of the recovery could be prevented either by strong intracellular Ca^{2+} ($[Ca^{2+}]_i$) buffering with 30 mM BAPTA or by using Ca^{2+}-free extracellular solution.

3. Simultaneous measurement of currents and Ca^{2+}-dependent fluorescence revealed a close correlation between the time constants of $[Ca^{2+}]_i$ decay and the slow component of NMDA-activated test current recovery.

4. During prolonged recordings, the transient inactivation was not related to irreversible NMDA-activated current run-down. After 25 min of recording with ATP-free intracellular solution, NMDA-activated currents in hippocampal neurones irreversibly decreased by $49 \pm 5\%$ while inactivation decreased by 8% ($n = 9$). Calyculin A and FK-506 (phosphatase inhibitors) significantly delayed run-down but did not modulate the transient inactivation.

5. In cerebellar granule cells that did not show run-down (4 mM MgATP in the pipette) the percentage of transient inactivation strongly decreased during 25 min of recording (from 28 ± 6 to $7 \pm 5\%$, $n = 15$).

6. In cell-attached recordings (5 μM NMDA in the pipette), elevation of $[Ca^{2+}]_i$ (application of 100 μM NMDA to the soma) caused a reversible reduction of single NMDAR channel open probability (NP_o) due to a decrease in the frequency of channel opening.

7. In inside-out patches, application of Ca^{2+} to the cytoplasmic side of the membrane caused a rapid and reversible decrease in NP_o (13 out of 29 patches). In the absence of run-down, the ability of Ca^{2+} to transiently inhibit NMDAR channel activity disappeared after 3–5 min of recording.

8. These results indicate that Ca^{2+}-induced transient inactivation of NMDAR currents develops independently from the run-down and suggest that a diffusible Ca^{2+}-dependent factor mediates NMDAR channel inactivation.

The *N*-methyl-D-aspartate subtypes of glutamate receptor (NMDAR) channels have a high Ca^{2+} permeability and provide voltage-dependent regulation of synaptic excitation in neurones of the vertebrate central nervous system (see review by Mayer & Westbrook, 1987). These features are essential for physiological and pathological processes such as synaptic long-term plasticity, neuronal migration during embryogenesis, development of synaptic connections, and neurodegeneration (see references in Zukin & Bennett, 1995). The function of this receptor is modulated by a number of regulatory sites on the external and internal parts of the plasma membrane (see review by Hollman & Heinemann, 1994).

* Present address to which correspondence should be addressed: Laboratoire de Neurobiologie Cellulaire, Institut Pasteur, 25 rue de Dr Roux, 75264 Paris, Cedex 15, France.

It is now well documented that the activity of NMDAR channels is negatively modulated by intracellular calcium ($[Ca^{2+}]_i$). Three main modulatory effects of Ca^{2+} on NMDAR channels have been described: (i) irreversible inhibition or run-down (Rosenmund & Westbrook, 1993*a*); (ii) irreversible acceleration of glycine-independent desensitization (Vyklický, 1993; Tong & Jahr, 1994) and (iii) reversible (transient) inactivation, a phenomenon which develops independently of the activation of the NMDA receptor (Mayer & Westbrook, 1985; Zorumski, Yang & Fischbach, 1989; Legendre, Rosenmund & Westbrook, 1993; Vyklický, 1993; Medina, Bregestovski & Ben-Ari, 1993; Medina, Filippova, Barbin, Ben-Ari & Bregestovski, 1994).

Transient inactivation by $[Ca^{2+}]_i$ seems to be an intrinsic property of the NMDAR channel because it has been reported for recombinant NMDA receptors expressed in HEK293 cells (Medina *et al.* 1995). Ca^{2+}-induced inactivation of the synaptic component of NMDA-activated currents was also recently described (Rosenmund, Feltz & Westbrook, 1995; Medina, Leinenkugel, Rovira, Ben-Ari & Bregestovski, 1995), which suggests that this phenomenon may play a role in negative feedback regulation of glutamate-induced excitation during synaptic transmission.

Mechanisms of Ca^{2+}-induced transient inactivation are not clear. This effect could be due either to a direct action of Ca^{2+} ions on specific sites of the NMDA receptor, or involve a Ca^{2+}-dependent intermediate system. In one study, application of Ca^{2+} to the cytoplasmic side of excised inside-out patches was ineffective (Rosenmund & Westbrook, 1993*b*), while in another study on the same preparation, transient inactivation of single NMDAR channels was reported to be similar to that seen in whole-cell configuration (Vyklický, 1993). A relatively slow development of Ca^{2+}-induced inactivation was observed during whole-cell (Legendre *et al.* 1993; Rosenmund & Westbrook, 1993*a*, *b*) and inside-out recording (Vyklický, 1993).

It has been proposed that Ca^{2+}-dependent transient inactivation occurs due to dissociation of a regulatory protein from the NMDAR channel upon Ca^{2+} binding (Rosenmund & Westbrook, 1993*b*). The channel can recover from inactivation as Ca^{2+} is removed and the regulatory protein rebinds. Ca^{2+}-mediated depolymerization of actin filaments results in loss of the regulatory protein and progression of the NMDAR channel to the run-down state (Rosenmund & Westbrook, 1993*b*). According to this model, transient inactivation is an intermediate state of the process which leads to Ca^{2+}-dependent and cytoskeleton-dependent 'run-down'. A major prediction is that transient inactivation and run-down should develop in succession, i.e. (i) the inactivation should disappear, if run-down occurs; and (ii) the inactivation should persist, if run-down is prevented. However, these consequences of the hypothesis have not been analysed in detail.

To understand better the properties of Ca^{2+}-induced transient inactivation we studied this phenomenon in cultured hippocampal neurones and cerebellar granule cells in the whole-cell configuration and on inside-out patches. Cerebellar granule cells were selected for two main reasons. Firstly, granule cells have a much smaller size than hippocampal neurones which allows better intracellular dialysis; secondly, they lack three Ca^{2+}-binding proteins: calcineurin, calbindin and parvalbumin (Heizmann & Hunziker, 1991), which are present in hippocampal neurones (Miettinen, Gulyas, Baimbridge, Jacobowitz & Freund, 1992). Comparative studies allowed us to conclude that these Ca^{2+}-binding proteins are not directly involved in the process of Ca^{2+}-induced inactivation. Our results also demonstrate that the run-down of the NMDA-activated current and Ca^{2+}-induced inactivation develop independently, i.e. the degree of Ca^{2+}-induced inactivation does not correlate with run-down of NMDA-activated currents and the ability of $[Ca^{2+}]_i$ to transiently inhibit NMDA-activated currents gradually disappears in conditions when run-down is absent. Based on these results we propose a model suggesting the existence of a diffusible Ca^{2+}-dependent factor which mediates NMDAR channel inactivation. The loss of this factor does not change the activity of the channel: it removes the ability of the channel to be inactivated by Ca^{2+}.

METHODS

Cell culture

The experiments were conducted on two types of primary neurone cultures prepared from hippocampi of 2-day-old rats (Wistar) and cerebella of 7- to 8-day-old rats.

Primary culture of hippocampal neurones. For preparation of dissociated neurones, rats were rapidly decapitated after cervical dislocation, and the hippocampi were removed from the brain and dissected free of meninges in cooled (6 °C) oxygenated phosphate-buffered saline (PBS) containing Ca^{2+} and Mg^{2+}. The hippocampi were then transferred into Ca^{2+}- and Mg^{2+}-free PBS, cut into small pieces and incubated with 0·3% (w/v) protease from *Aspergillus oryzae* (Type XXIII; Sigma) and 0·1% (w/v) DNase (Type I; Sigma) for 20 min at 25 °C. The tissue was washed and triturated using fire-polished pipettes in Ca^{2+}- and Mg^{2+}-free PBS solution with 0·05% DNase. After a brief centrifugation, the cell pellet was resuspended in culture medium and plated at a density of 20000–80000 cells cm^{-2}. Growth medium contained 8% NU serum (Becton Dickinson, Franklin Lakes, NJ, USA) and 92% minimal essential medium (MEM; Gibco) supplemented with penicillin (5 U ml^{-1}) and streptomycin (5 μg ml^{-1}). Glass coverslips were coated with poly-L-lysine (MW range, 30000–70000) in 0·1 M borate buffer at pH 8·9 (Sigma).

Primary culture of granule neurones from rat cerebellum. The brain was removed from 7- to 8-day-old Wistar rats which had been killed by cervical dislocation and rapidly decapitated. The dissection of the cerebellum formation was performed in Ca^{2+}- and Mg^{2+}-free PBS supplemented with 0·6% (w/v) glucose. The tissue was incubated for 20 min at room temperature (19–22 °C) with 0·2% (w/v) trypsin (bovine pancreas; Sigma) and 0·1% (w/v) DNase. The action of trypsin was stopped with 1% (w/v) soybean trypsin inhibitor. The tissue was dispersed with a fire-narrowed Pasteur pipette in Dulbecco's modified Eagle's medium (DMEM; Gibco) supplemented with 0·05% (w/v) DNase. After a brief

centrifugation, the cell pellet was resuspended in culture medium (see below). Tissue culture dishes were coated for 12 h with 10 μg ml^{-1} poly-L-lysine in 0·1 M borate buffer at pH 8·9. The cells were seeded at a density of 150 000 cells cm^{-2} in a culture medium (DMEM with 20 g l^{-1} glucose, 5 U ml^{-1} penicillin and 5 μg ml^{-1} streptomycin) supplemented with 10% NU serum.

Electrophysiological recording and analysis

Whole-cell recording. Experiments were performed in whole-cell voltage-clamp mode on hippocampal and cerebellar neurones after 1–3 weeks in culture. Currents were recorded using EPC-9 and EPC-7 amplifiers (HEKA Electronik, Lambrecht, Germany) and stored on digital tape using a DTR 1201 recorder (Bio-Logic, Claix, France). The internal solution (unless otherwise mentioned in the text) contained (mM): CsCl, 100; caesium gluconate, 80; Cs_4BAPTA, 1·1; $CaCl_2$, 0·2; Cs-Hepes, 10; Mg-ATP, 4·0; GTP, 0·6; and creatine phosphate, 6·0; pH 7·2. Osmolarity was adjusted to 310 mosmol l^{-1} by adding caesium gluconate. The resistance of recording borosilicate glass pipettes was 3–6 MΩ and series resistance was in the range of 10–30 MΩ. The external solution contained (mM): NaCl, 180; KCl, 1; $CaCl_2$, 2; Na-Hepes, 10; glucose, 2; and glycine, 0·01; pH 7·4. Osmolarity was adjusted to 340 mosmol l^{-1} by adding NaCl.

The holding potential (V_h) was −60 mV in all experiments on hippocampal neurones and −50 mV in cerebellar granule cells. To test the activity of the NMDAR channels, short (50–150 ms) applications of external solution containing 50–300 μM NMDA were made every 10 s using micropipettes (tip diameter, 2 μm) and Picospritzers (General Valve Corporation, Fairfield, NJ, USA) as previously described (Medina *et al.* 1994). To increase $[Ca^{2+}]_i$ and to induce Ca^{2+}-dependent inactivation of the NMDA-activated currents, long (5–15 s) conditioning applications of NMDA were applied using the same micropipette or a fast perfusion system.

For analysis, data were filtered at 1–3 kHz and digitized at 5–10 kHz using pCLAMP 6 software (Axon Instruments), a Labmaster DMA board (DIPSI, France) and an IBM AT computer (Intersys, USA).

The degree of inactivation was estimated using the equation $(I_0 - I)/I_0$, where I_0 is the peak amplitude of NMDA-activated test currents before application of the conditioning pulse of NMDA, and I is the peak amplitude of test current 4 s after the conditioning pulse. The charge (Q) passing through the cell during conditioning applications of NMDA was estimated as the integral of agonist-induced current using pCLAMP 6 software.

Single-channel current recording. Single-channel NMDA-activated currents were recorded in cell-attached and inside-out configurations from hippocampal and cerebellar neurones after 10–20 days in culture. Polished patch pipettes (2–6 MΩ) containing 5 μM NMDA and 10 μM glycine in Ca^{2+}-free external solution buffered with 1–5 mM BAPTA (pH 7·4) were used. Mg^{2+} (5 μM) was included routinely in pipette solutions to identify NMDAR channel currents: flickering augmentation at hyperpolarization (Nowak, Bregestovski, Ascher, Herbet & Prochiantz, 1984). For elevation of $[Ca^{2+}]_i$ during cell-attached recording pressure pulses of NMDA (5–10 s, 50 μM) were applied to the surface of the neurones. Two to five seconds before obtaining the inside-out patch the external solution was exchanged for Ca^{2+}-free solution containing 1–5 mM BAPTA.

Single-channel currents were recorded at 3 kHz using an EPC-9 amplifier (HEKA Electronik) and stored on a digital data recorder DTR 1201 (Bio-Logic). Replayed currents were digitized at 15 kHz and analysed on an IBM AT computer using pCLAMP 6 software. Briefly, after acquisition the single-channel traces were analysed in manual mode using the FETCHAN program to avoid including artefacts into idealized data. Open probability (NP_o) and other kinetic parameters were calculated using the pSTAT program of pCLAMP 6 software. NP_o was calculated as $NP_o = t_o/t_i$, where t_o is the total open time for the level under consideration, t_i is the time interval over which P_o is measured.

Measurements of $[Ca^{2+}]_i$-dependent fluorescence

The monitoring of changes in $[Ca^{2+}]_i$ were performed on hippocampal neurones loaded with the Ca^{2+}-sensitive dye fluo-3 (10 μM; Molecular Probes) included in the patch recording pipette. A confocal laser-scanning microscope (MRC-600, BioRad, Hemel Hempstead, Herts, UK) equipped with an argon–krypton laser and photomultiplier was combined with an Axioscope Karl Zeiss microscope (×40 water-immersion objective lens). Excitation was delivered at 488 nm and emmission intensity was measured at > 500 nm. The subsequent modification of the program 'SOM' (BioRad) was used to record thirty-two successive images with a 2 s interval. Image acquisition and whole-cell recording were simultaneously performed.

The changes in fluorescence were quantified off-line using the program Fluo (IMSTAR, Paris, France). A specified portion of the cell was outlined on one of the images and quantification of the intensity of the fluorescence was done within these limits on all the images (see Fig. 2). Changes in fluorescence were calculated using the equation $(F - F_{min})/F_{min}$, where F_{min} is the fluorescence of the first image (background level) and F is the fluorescence of the corresponding (current) image.

All results are presented as mean values ± S.E.M. Data were compared statistically by Student's t test. Statistical significance was determined at the 5% level.

RESULTS

Ca^{2+}-induced inactivation of NMDA-activated currents in cultured neurones from rat hippocampus

The properties of Ca^{2+}-induced transient inactivation of NMDA-activated currents were studied using the double-pulse experimental protocol of NMDA application. At a V_h of −60 mV, the NMDA test pulses (50 ms) repeatedly applied at 5–10 s intervals induced stable inward currents with amplitudes of 200–800 pA. A conditioning (3–10 s) application of NMDA reversibly reduced the amplitudes of the NMDA test responses. The recovery time course was estimated by varying the interval (from 0·3 to 60 s) between the end of the conditioning pulse and the following NMDA test pulse (Fig. 1*A* and *B*).

When the intracellular solution contained a weak Ca^{2+} buffer (1·1 mM BAPTA + 0·25 mM Ca^{2+}; free $[Ca^{2+}]$, 10^{-8} M) the recovery of test current amplitudes after the conditioning NMDA application developed in two distinct phases with time constants τ_1 and τ_2 of 0·57 ± 0·12 and 37·6 ± 8·9 s, respectively ($n = 5$; Fig. 1*A*). The first component of this process reflects the recovery of the NMDA receptor from agonist-induced desensitization. This process is relatively fast and is completed within 3–5 s of the conditioning NMDA application (Mayer, Vyklický & Westbrook, 1989; Sather, Dieudonne, MacDonald & Ascher, 1992). The second component was abolished by using recording pipettes with

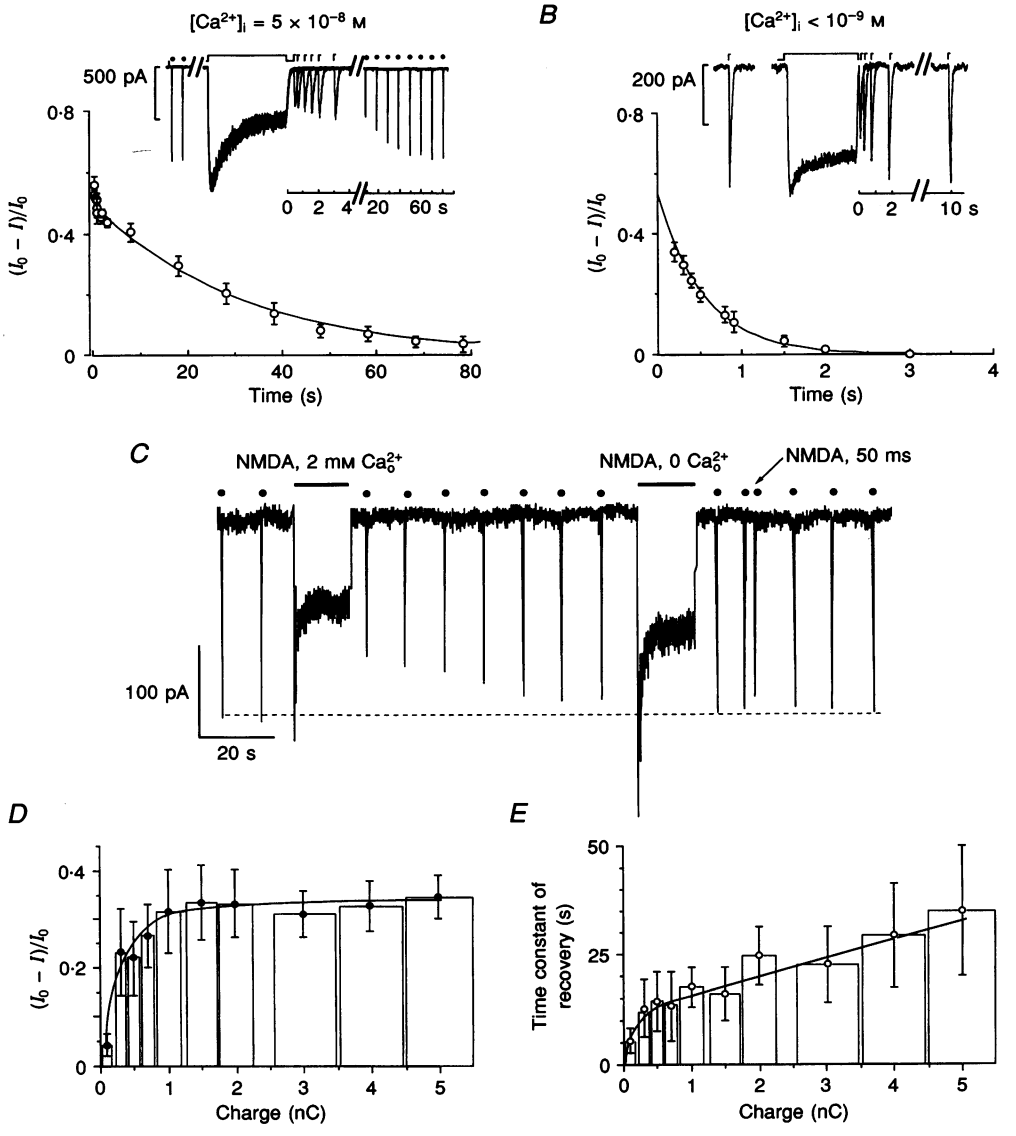

Figure 1. Ca^{2+}-induced inactivation of NMDAR channels in cultured hippocampal neurones

Whole-cell recording at $V_h = -60$ mV. *A*, recovery of NMDAR channels from desensitization in the presence of a weak intracellular Ca^{2+} buffer (1·1 mM BAPTA + 0·2 mM Ca^{2+}, free $[Ca^{2+}] = 10^{-8}$ M). Mean results from 5 experiments. Mean values were fitted using a least-squares double-exponential fitting procedure ($\tau_1 = 0{\cdot}6$ s, $\tau_2 = 39$ s). Inset, examples of double-pulse recording for estimation of the time course of recovery from desensitization. Brief (50 ms) test pulses of 70 μM NMDA (•, Γ) were applied using a micropipette at different intervals after conditioning pulses (continuous line). Six traces are superimposed. Note the two time scales for better illustration of double-exponential recovery of the NMDA-activated currents. *B*, recovery of NMDAR channels from desensitization in the presence of a strong intracellular Ca^{2+} buffer (10 mM BAPTA). Plots represent mean results from 5 experiments. Data were fitted using a single exponential with a time constant τ of 0·8 s. Inset, traces of 4 superimposed records. *C*, the slow component of NMDAR channel recovery is $[Ca^{2+}]_o$ dependent. Test pulses of NMDA (•) were applied using a micropipette containing a Ca^{2+}-free solution. Conditioning pulses of NMDA (bars) were applied using a fast perfusion system with a Ca^{2+}-free solution or a solution containing 2 mM Ca^{2+}, as indicated above the trace. Dashed line indicates mean value of NMDA-activated test currents before the first conditioning application of NMDA. Note that in Ca^{2+}-free solution the conditioning application of NMDA did not decrease the amplitude of test currents. *D* and *E*, the degree of Ca^{2+}-induced inactivation (*D*) and the time constant of the recovery of NMDA-activated test currents from inactivation (*E*) as a function of charge (*Q*) passed through the NMDAR channel during conditioning application of agonist. The means of results from 18 experiments are presented. In each experiment at least 3 conditioning pulses of NMDA with different durations were applied. The charge was calculated as the integral of the NMDA conditioning current. The width of the columns corresponds to the ranges of charges averaged from different cells. The degree of inactivation was calculated as $(I - I_0)/I$ where I_0 is the amplitude of the NMDA-activated test current before application of the conditioning pulse of NMDA and I is the amplitude of the NMDA test response 4 s after the conditioning application of NMDA, i.e. when the first phase of the recovery was complete.

solutions containing strong Ca^{2+} buffers (from 10 to 30 mM BAPTA in different cells, $n = 5$; Fig. 1*B*) or in Ca^{2+}-free external solution ($n = 9$; Fig. 1*C*). This phase reflects the recovery of NMDAR channels from transient Ca^{2+}-induced inactivation (Medina *et al.* 1994, 1995).

As illustrated in Fig. 1*D* the degree of Ca^{2+}-induced inactivation depends on the charge (Q) passed through the NMDAR channels during conditioning applications. At a $[Ca^{2+}]_o$ of 2 mM the degree of inactivation increased from $4 \pm 1\%$ when Q was $0{\cdot}1 \pm 0{\cdot}05$ nC to $31 \pm 9\%$ when Q was $1 \pm 0{\cdot}2$ nC ($n = 18$). Further elevation of Q (from 1 to 5 nC) did not significantly change the degree of inactivation.

The kinetics of the recovery also depended on the conditioning charge (Fig. 1*E*). As Q was increased from 0·1 to 5 nC, the time constant of recovery from Ca^{2+}-induced inactivation increased from 5 ± 3 to 35 ± 15 s ($n = 18$). Such slow kinetics could reflect the slow time course of $[Ca^{2+}]_i$ recovery after conditioning applications. To evaluate the relation between the dynamics of $[Ca^{2+}]_i$ and its inhibitory action on NMDAR channels, simultaneous monitoring of whole-cell currents and Ca^{2+}-sensitive fluorescence using fluo-3 and a confocal microscope was done.

Correlations between $[Ca^{2+}]_i$ and the degree of Ca^{2+}-induced inactivation of NMDA-activated currents

Figure 2*A* shows that conditioning NMDA pulses locally applied to the soma of the hippocampal neurones induced a transient increase in fluorescence which slowly declined to the basal level. As demonstrated in Fig. 2*B*, the time course of fluorescence changes and of NMDA-activated test currents coincided.

Table 1 summarizes the estimated kinetic recovery of Ca^{2+}-dependent fluorescence and NMDA-activated current amplitudes from thirteen experiments. The time of recovery varied nearly 10-fold. In each case, however, the time constants of the fluorescence decay and recovery of NMDA-evoked test responses after the conditioning application were similar. The correlation coefficient between these values is 0·97.

These results suggest that the time course of NMDA-activated current recovery from transient inactivation reflects the kinetics of $[Ca^{2+}]_i$ decay to the basal level, suggesting that modulation of NMDAR channel activity is controlled by the Ca^{2+} concentration and is a relatively fast process.

Ca^{2+}-induced inactivation of NMDA-activated currents in hippocampal neurones during prolonged whole-cell recording

Figures 3 and 4 characterize the Ca^{2+}-induced inactivation of the NMDA-evoked currents during long-lasting whole-cell recording from hippocampal neurones using different intracellular solutions: (i) ATP-free solution (in the absence of ATP, GTP and creatine phosphate); (ii) ATP-free solution containing calyculin A (an inhibitor of phosphatases type 1 and type 2A) or FK-506 (an inhibitor of calcineurin, a Ca^{2+}–calmodulin-dependent phosphatase type 2B); (iii) ATP-supported solution (see Methods). In records with ATP-free intracellular solutions the amplitude of the NMDA-activated test currents decreased progressively and reached a steady state ($51 \pm 5\%$, $n = 9$) after 20 min of recording (Fig. 3*A* and *B*). The half-maximal run-down was reached after 4–10 min (mean value, about 8 min) (Fig. 3*B*).

Table 1. Time constants of the recovery of $[Ca^{2+}]_i$ (τ_{Ca}) and responses to NMDA (τ_{NMDA}) after conditioning applications of NMDA during simultaneous recording of Ca^{2+}-dependent fluorescence and NMDA-activated currents (for details, see Methods)

Expt no.	τ_{Ca} (s)	τ_{NMDA} (s)
1	13	5
2	17	25
3	18	11
4	20	18
5	22	16
6	25	28
7	30	25
8	35	27
9	42	30
10	45	38
11	65	60
12	68	74
13	104	94

The degree of transient inactivation of the NMDA-activated test currents did not correlate with that of run-down. In the experiment shown in Fig. 3*A* the degree of inactivation decreased by only 12% (from 45 to 33%) after 27 min of recording while run-down reached 55% of initial values after only 15 min of recording. On average, Ca^{2+}-induced inactivation decreased by only 8% during the first 25 min of the experiment (from $36 \pm 6\%$ at the 3rd min of the recording to $28 \pm 2\%$ after 20–25 min) (Fig. 3*C*).

The inclusion of 100 nM calyculin A or 500 nM FK-506 in the pipette significantly delayed the run-down of the NMDA-activated currents (Fig. 3*B*). After 13 min of recording, the difference between the control value (ATP-free solution) ($66 \pm 7\%$, $n = 9$) and those obtained in the presence of calyculin A ($98 \pm 8\%$, $n = 5$, $P < 0{\cdot}05$) or FK-506 ($90 \pm 5\%$, $n = 5$, $P < 0{\cdot}05$) became significant. In contrast, as illustrated in Fig. 3*C* neither calyculin A nor FK-506 significantly modulated the degree of transient Ca^{2+}-induced inactivation of NMDA-activated currents.

The inclusion of ATP, GTP and creatine phosphate in the intracellular solutions induced a slight increase in NMDA-activated test currents during the first 2–3 min after establishing whole-cell configuration ($108 \pm 3\%$, $n = 25$) and then currents remained stable for up to 55 min ($103 \pm 5\%$ after 25 min of recording, $n = 25$; $95 \pm 8\%$ after 50 min, $n = 7$) (Fig. 4*A* and *B*).

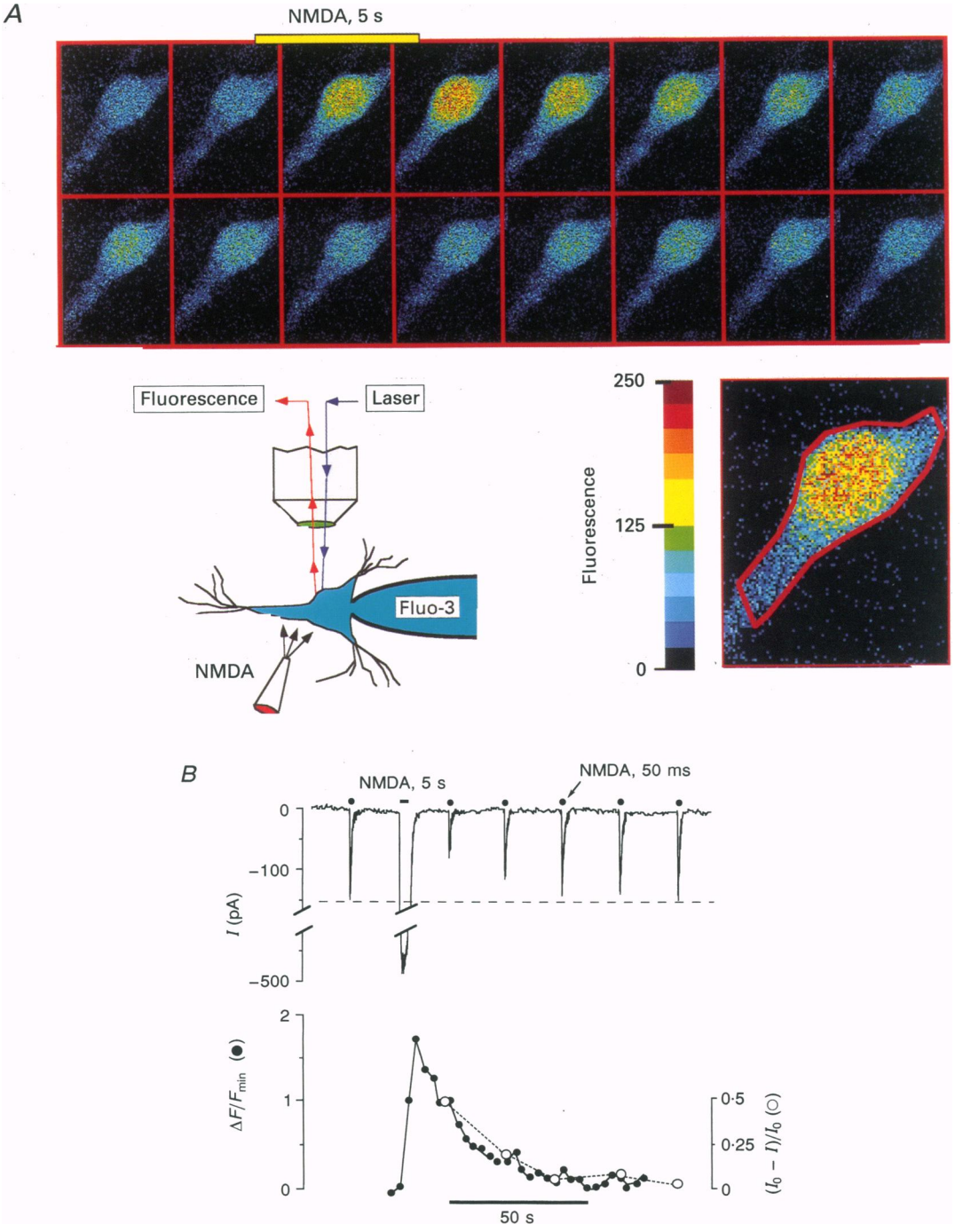

Figure 2. Correlation between $[Ca^{2+}]_i$ and inactivation of the NMDA-activated currents in hippocampal neurones

Simultaneous measurement of the Ca^{2+}-dependent fluorescence and NMDA-activated currents. The Ca^{2+}-sensitive fluorescent dye fluo-3 (10 μM) was loaded using a whole-cell recording pipette (V_h, −50 mV). NMDA (100 μM) was pressure applied to the soma of the neurone through a pipette with a diameter of 1–2 μm as illustrated by the scheme in the bottom of panel *A*. *A*, example of successive images obtained every 3 s. A 5 s conditioning application of NMDA was started after screening of the second image. Note the transient increase of the Ca^{2+}-dependent fluorescence induced by application of the NMDA. Red outline in the single image marks the area from which fluorescence was calculated. *B*, simultaneous recording of whole-cell currents (top) and of Ca^{2+}-dependent fluorescence (bottom) during application of NMDA. Note the similar recovery times from inactivation of fluorescence and NMDA-activated test currents. Fluorescence is presented as $(F - F_{min})/F_{min}$, where F_{min} is the fluorescence of the first image (background level) and F is the fluorescence of the corresponding (current) image.

In the majority of neurones which showed stable responses to NMDA, the degree of Ca^{2+}-induced inactivation did not change significantly during prolonged recordings ($n = 22$). As illustrated in Fig. 4*A*, after a conditioning application at the 3rd and 35th min of recording, NMDA-activated test currents were similarly inhibited (27 and 25%, respectively) and the time course of recovery to control values, 40–50 s, was unchanged. On average, after 2 and 30 min of whole-cell recording, conditioning charges of 1–1·5 nC caused inactivation by 35 ± 3 and 33 ± 4%, respectively ($n = 22$). For longer recordings (50 min) a weak run-down (95 ± 7%, $n = 5$), was accompanied by a similarly small decrease in the degree of Ca^{2+}-induced inactivation (30 ± 4%, $n = 5$) (Fig. 4*B*).

However, in three neurones a different behaviour was observed: in the absence of run-down, the degree of Ca^{2+}-induced inactivation continuously decreased and after 45–60 min of recording, it disappeared completely. In the experiment illustrated in Fig. 4*C*, the degree of test current inactivation decreased from 39% at the 3rd min of whole-cell recording to 17% at the 25th min and disappeared completely after 50 min.

These observations suggest that the degree of Ca^{2+}-induced transient inactivation of the NMDA-activated currents does not always correlate with run-down of NMDAR channels.

The fact that in some hippocampal neurones, during long-lasting recording, the ability of $[Ca^{2+}]_i$ to transiently inhibit NMDA-activated currents disappeared in the absence of run-down, raises the possibility that a slow washout of some Ca^{2+}-sensitive component is involved in transient inactivation. To check this suggestion, we used two experimental models: (i) small cerebellar granule cells, which allow better intracellular dialysis of the soma; and (ii) inside-out patches, to allow direct application of Ca^{2+} to the cytoplasmic side of the membrane.

The Ca^{2+}-induced inactivation of NMDA-activated currents in rat cerebellar granule neurones

Figure 5 summarizes the results of the analysis of NMDA-activated whole-cell currents recorded from cerebellar granule neurones. Brief (50 ms) test pulses of NMDA generated inward currents with peak amplitudes of 50–300 pA ($V_h = -50$ mV). As for hippocampal neurones, conditioning NMDA pulses (3–7 s) induced reversible inhibition of NMDA-activated test currents with a slow (10–30 s) recovery. This effect was observed in twenty-five out of thirty-four granule cells during the first 10 min of whole-cell recording. In the remaining nine neurones, transient inactivation was absent from the very beginning of the experiment.

Several lines of evidence suggest that this inhibition was a Ca^{2+}-dependent process. First, slowly recovering inhibition

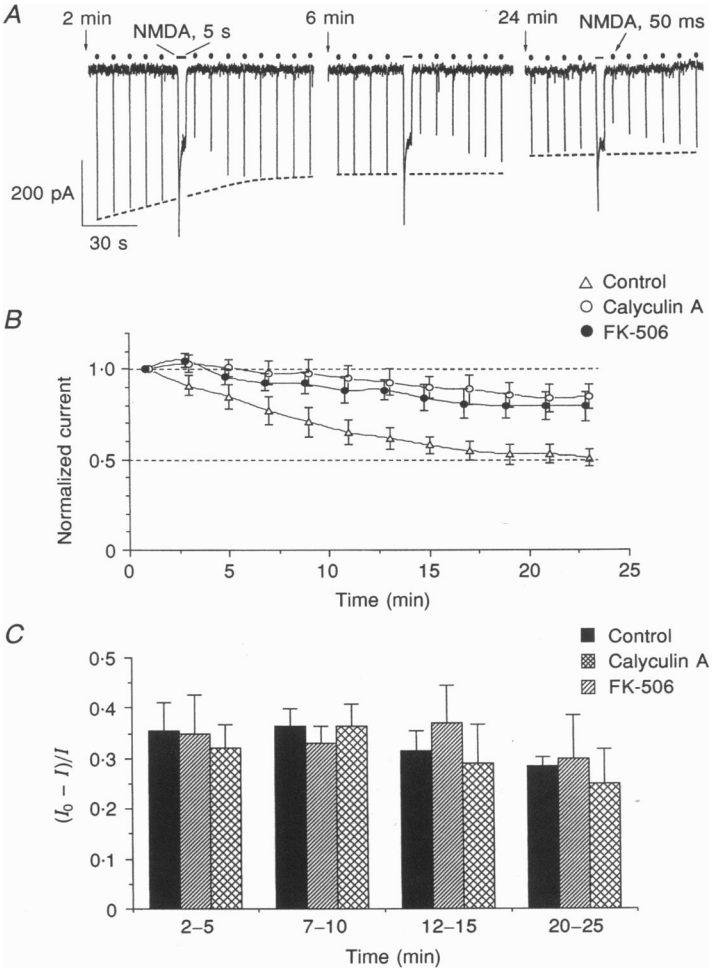

Figure 3. Ca^{2+}-induced inactivation of the NMDA-activated currents in hippocampal neurones during long-lasting whole-cell recording in absence of ATP, GTP and creatine phosphate in intracellular solution

$V_h = -60$ mV. *A*, traces of whole-cell currents after 2, 6 and 24 min of experiment. The NMDA test pulses (50 ms) (•) were applied every 10 s. Conditioning (5 s) pulses of NMDA (bars) were applied every 5–10 min. Following the conditioning application of NMDA the first test pulse was applied after a 4 s interval. The total charges (Q) for conditioning NMDA pulses after 2, 6 and 24 min of whole-cell recording were 1·27, 1·24 and 1·13 nC, respectively. *B* and *C*, the phosphatase inhibitors calyculin A and FK-506 modulate the rate of run-down without affecting the transient Ca^{2+}-induced inactivation. NMDA-activated test current amplitude (*B*) and the degree of Ca^{2+}-induced inactivation (*C*) are shown for control ($n = 9$) and after addition of calyculin A (100 nM; $n = 5$) or FK-06 (500 nM; $n = 5$). Data are summarized from 5 to 9 neurones. In *B*, in each experiment the mean of 8–12 successive test current amplitudes (records of 2 min duration) were calculated and then all values were normalized to the first one.

was not observed at positive potentials ($V_h = +50$ mV), when the driving force for Ca^{2+} influx is negligible (Fig. 5*A*, $n = 18$). Second, reduction of $[Ca^{2+}]_o$ to 0–0·1 mM reversibly prevented, or decreased the inhibitory effect of conditioning NMDA pulses (Fig. 5*B*, $n = 6$). Third, this effect was absent when 30 mM BAPTA was present in the intracellular solution (data not shown, $n = 5$).

The dependence of the degree of inactivation on the conditioning charge passed through NMDAR channels was similar to that for hippocampal neurones (Fig. 5*C*). The maximal degree of inactivation increased with elevation of $[Ca^{2+}]_o$. It was 24 ± 4% for a $[Ca^{2+}]_o$ of 2 mM ($n = 15$) and 36 ± 5% ($n = 10$) for a $[Ca^{2+}]_o$ of 5 mM. Maximal inactivation in granule cells was reached at a lower value for

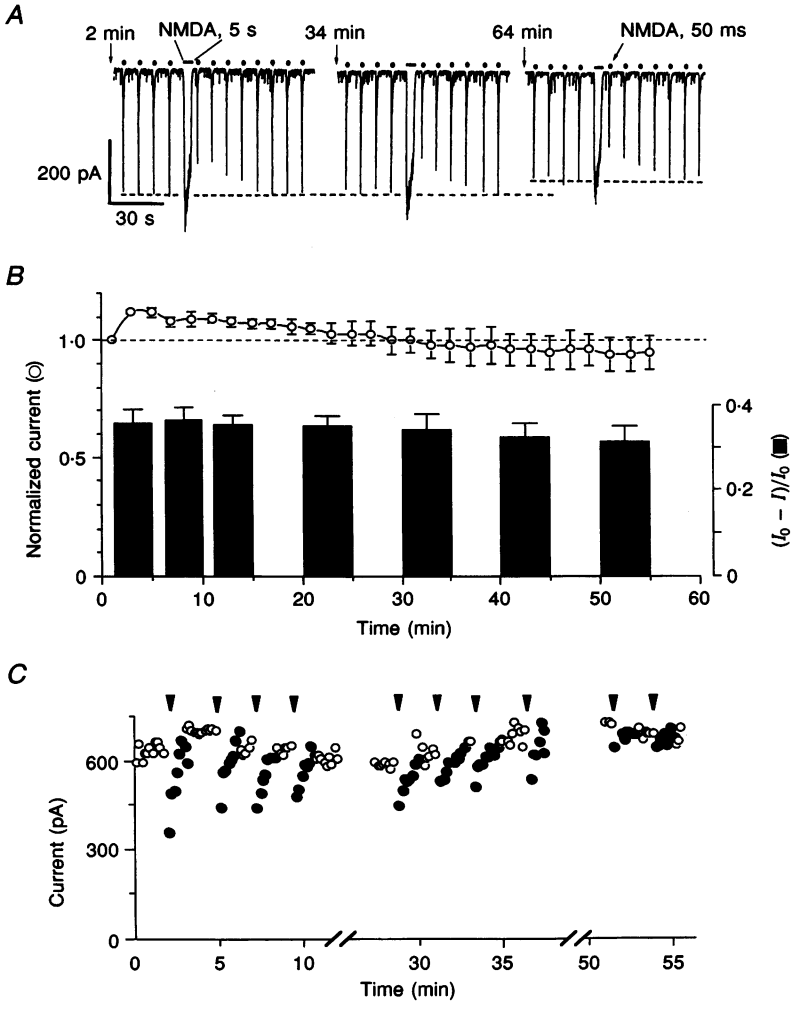

Figure 4. Ca^{2+}-induced inactivation of the NMDA-activated currents in hippocampal neurones during long-lasting whole-cell recording using ATP-supported (4 mM Mg-ATP) intracellular solution

$V_h = -60$ mV. *A*, traces of whole-cell currents. Experimental protocol similar to that of Fig. 3*A*. The degrees of Ca^{2+}-induced inactivation after 2, 34 and 65 min of recording were, respectively, 25, 30 and 31% and the total Q values of conditioning NMDA pulses were 1·9, 1·87 and 1·57 nC, respectively. Dashed lines have the same significance as Fig. 1*C*. *B*, plot of the average NMDA-activated test current amplitude (○) and of the degree of the Ca^{2+}-induced inactivation (columns) during prolonged whole-cell recording. The results corresponding to the first 30 min of the recording were from 22 cells. Results from longer duration recordings (40–55 min) are averaged from 5 cells as recordings were terminated at various times thereafter. The mean ± S.E.M. of normalized test currents were obtained as described in Fig. 3. Columns represent means ± S.E.M. of the degree of Ca^{2+}-induced inactivation measured during intervals of time which correspond to the width of the columns. Dashed line indicates the amplitude of NMDA-activated test currents at the beginning of the experiment (100%). *C*, Ca^{2+}-induced transient inactivation can disappear during long-lasting recording in the absence of run-down. An example of 1 of 3 experiments is illustrated. ○, amplitude of the NMDA-activated test currents. Times of the NMDA conditioning applications are shown by arrowheads. For better visualization of the Ca^{2+}-induced inactivation, 8 test current amplitudes following conditioning applications of NMDA are shown (●).

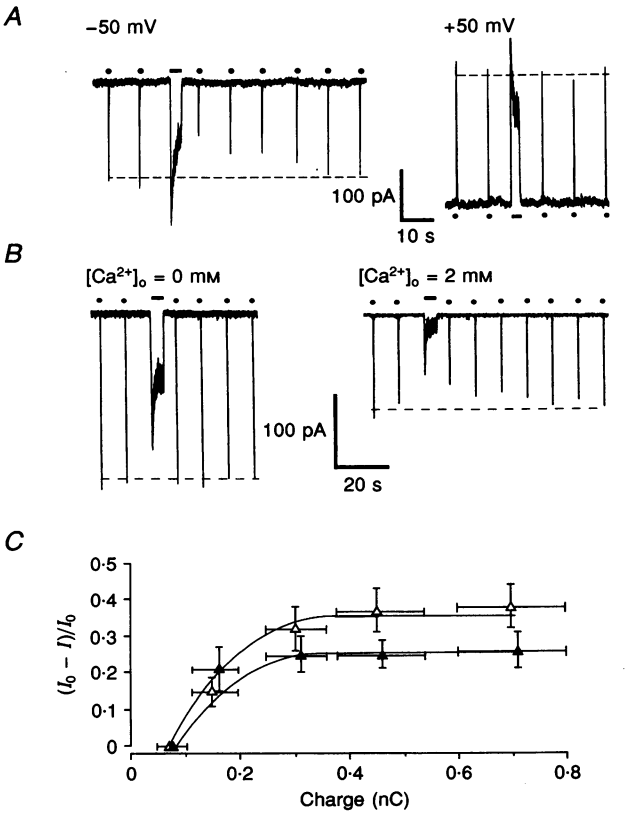

Figure 5. Ca^{2+}-induced inactivation of the NMDAR channels in cerebellar granule cells

The test pulses of NMDA (•) were applied using a micropipette. Conditioning pulses of NMDA (bars) were applied using a fast perfusion system. *A*, NMDA-activated currents at $V_h = -50$ mV (left trace) and $V_h = +50$ mV (right trace) in the presence of 2 mM Ca_o^{2+}. Note that the test currents inactivate at −50 mV but not at +50 mV. The ratio of steady-state/peak of conditioning current is also different (0·38 at −50 mV and 0·54 at +50 mV). *B*, NMDA-activated currents at $[Ca^{2+}]_o = 0$ mM (left trace) and $[Ca^{2+}]_o = 2$ mM (right trace). Note the absence of test current inactivation in the Ca^{2+}-free external solution. The ratios of steady-state/peak of the conditioning current were 0·48 in Ca^{2+}-free solution and 0·19 at 2 mM Ca_o^{2+}. Dashed lines in *B* and *C* have the same significance as in Fig. 1*C*. *C*, dependence of the degree of Ca^{2+}-induced inactivation on charge passed through NMDAR channels during conditioning application of NMDA at different $[Ca^{2+}]_o$. The degree of inactivation and charge passed through the NMDAR channel were calculated as described in Fig. 1*D*. The horizontal bars correspond to the ranges of Q values included in calculation of each point. The mean results from 10 and 15 experiments (in the presence of 2 mM (▲) and 5 mM Ca_o^{2+} (△), respectively) are presented.

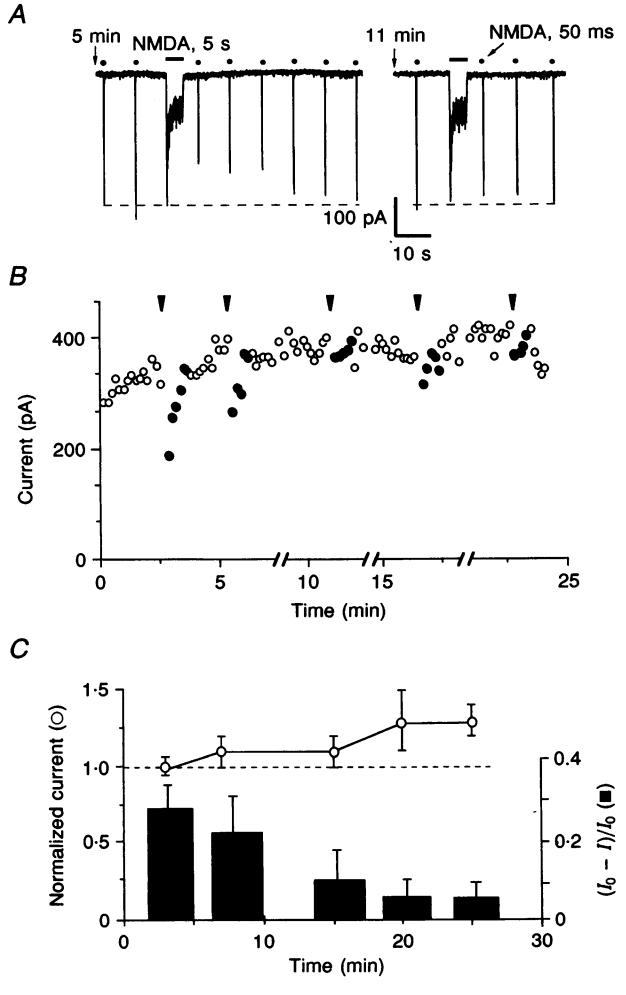

Figure 6. Ca^{2+}-induced inactivation of NMDA-activated test currents in cerebellar granule neurones during long-lasting whole-cell recording

The test (•) and conditioning (bars) applications of 100 μM NMDA were performed using a fast perfusion system in the presence of 2 mM Ca_o^{2+}. *A*, inactivation of the NMDA-activated test currents (•) induced by conditioning application of NMDA (bars) after 5 and 11 min of whole-cell recording at $V_h = -50$ mV. The degrees of inactivation were 47 and 8% respectively, and the total Q values of the conditioning NMDA pulses were 0·65 and 0·76 nC, respectively. Dashed lines have the same significance as in Fig. 1*C*. *B*, transient inactivation during whole-cell recording. Step-by-step presentation of NMDA-activated test current amplitudes in the experiment depicted in Fig. 6*A*. For better visualization of the degree of the Ca^{2+}-induced transient inactivation, 5 test current amplitudes (○) following conditioning applications of NMDA are shown (●). Arrowheads indicate the times of the conditioning applications of NMDA. Note the stable level of the NMDA-activated test current amplitude during the 25 min of recording and the disappearance of the transient Ca^{2+}-induced inactivation after 11 min of recording. *C*, average NMDA-activated test current amplitude (○) and degree of the Ca^{2+}-induced inactivation (columns) during prolonged whole-cell recording. The results of 14 experiments are presented. The average values were calculated using the same procedure as in Fig. 3*B*. Dashed line has the same significance as in Fig. 4*B*.

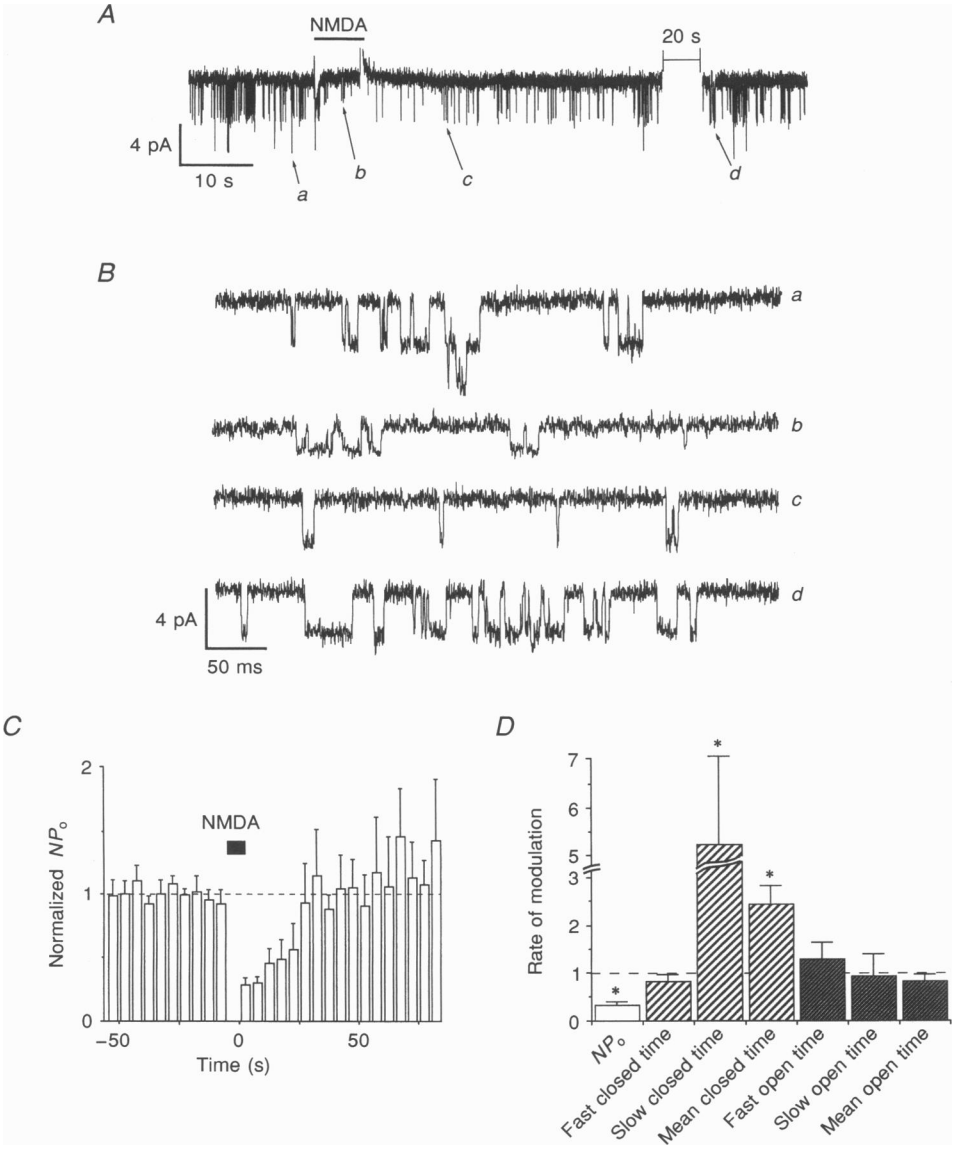

Figure 7. $[Ca^{2+}]_i$-dependent modulation of single NMDAR channels in cell-attached configuration
Recording pipette contained Ca^{2+}-free external solution with 10 μM NMDA, 10 μM glycine, 5 μM Mg^{2+} and 5 mM BAPTA. *A*, single-channel currents recorded in cell-attached configuration at a pipette potential of 0 mV. The resting potential was about −45 mV. Slow time base. To increase $[Ca^{2+}]_i$, NMDA was pressure applied to the soma of the neurone using a micropipette containing 50 μM NMDA. The duration of NMDA application is indicated by the bar. Note that during the application of NMDA the amplitude of the single-channel NMDA-activated currents decreased and progressively recovered to the control values by 3 s after the NMDA application. The frequency of the NMDAR channel opening also decreased and recovered to the control value within 30–50 s. For display the traces were digitized at 1 kHz. *B*, fast time base traces illustrating the single NMDAR channel current openings at times indicated in Fig. 7*A* by *a*, *b*, *c* and *d*. The traces were digitized at 10 kHz. *C*, the NMDAR channel open probability (NP_o) modulation by increases in $[Ca^{2+}]_i$ during conditioning NMDA application. Columns represent mean values from 5 cell-attached patches. The results of each experiment were normalized to the mean NP_o values (dashed line) before NMDA application. *D*, the effect of $[Ca^{2+}]_i$ on the kinetic parameters of NMDAR channels. Mean results from 5 experiments. Columns represent the ratio between the control value (results of analysis of 20 s records before application of NMDA; dashed line) and that obtained from records 20 s after NMDA application. The fast closed time, slow closed time, fast open time and slow open time are the time constants which describe the closed and open time distribution histograms. Time constants were obtained using least-squares double-exponential fitting procedures (see Methods). Statistical significance (*) was established using a Student's *t* test ($P < 0{\cdot}05$).

Q than in hippocampal neurones (compare Figs 1C and 5C), which probably reflects the difference in cell size.

Altogether, these data demonstrate that NMDAR channels in cerebellar granule cells possess Ca^{2+}-induced transient inactivation with properties similar to that described for hippocampal neurones.

Ca^{2+}-induced inactivation of NMDA-activated current in granule neurones during prolonged whole-cell recording

In granule cells, as in hippocampal neurones, the run-down and Ca^{2+}-induced inactivation of NMDA-activated currents were compared in the presence of ATP-supported internal solutions (see Methods) and at 2 or 5 mM Ca_o^{2+}.

In contrast to hippocampal neurones, in all granule cells which did not show run-down ($n = 15$ out of 34), Ca^{2+}-induced inactivation either completely disappeared or gradually decreased during 10–20 min of recording.

Application of a conditioning NMDA pulse in the 5th min of recording resulted in an inhibition of test currents by 34%, while 6 min later a conditioning application caused only 7% inhibition of NMDA test responses (Fig. 6A). Disappearance of Ca^{2+}-induced inactivation is shown in Fig. 6B. In this cell the amplitude of NMDA-induced currents was elevated by 30% during the first 5 min of the recording and it was then stable until the end of experiment. Conditioning NMDA pulses applied at the 3rd and 6th min of recording caused inactivation by 55 and 30%, respectively. Upon further conditioning applications, Ca^{2+}-induced inactivation was either very weak or absent. Similar effects were observed in fourteen other cells. On average, for this group of neurones, the degree of Ca^{2+}-induced inactivation decreased from 28 ± 6 to 7 ± 5% during 25 min of recording ($n = 15$; Fig. 6C). In the remaining nineteen cells tested, which showed run-down even in the presence of ATP-supported intracellular solution, Ca^{2+}-induced transient inactivation was either absent from the beginning of the recording or gradually decreased.

These data demonstrate that in granule neurones, in the absence of run-down, Ca^{2+}-induced inactivation of NMDA-activated currents decreases during prolonged whole-cell recording, i.e. NMDAR channels gradually become Ca^{2+} insensitive.

Ca^{2+}-induced inactivation of NMDAR channels in membrane patches of hippocampal neurones

Direct evidence for wash out of NMDAR channel sensitivity to $[Ca^{2+}]_i$ was obtained in experiments using excised inside-out patches.

Single-channel current identification. Figures 7 and 8 show representative single-channel currents recorded in cell-attached and inside-out configurations, when the patch pipette contained 5 μM NMDA, 10 μM glycine and 5 μM Mg^{2+}. These currents were characterized by bursts of short openings whose flickering frequency increased at hyperpolarization and decreased on depolarization. On recording from excised inside-out patches, single-channel current amplitude was a linear function of the membrane potential. Single-channel conductance, revealed from current–voltage relations in the range of −50 to 50 mV, varied from 55 to 75 pS (65 ± 3 pS, $n = 12$). Channels with this conductance were absent when recording with an NMDA-free pipette solution. Thus, these currents had typical features of earlier described NMDAR channels (Nowak *et al.* 1984; Ascher & Nowak, 1988; Ascher, Bregestovski & Nowak, 1988; Gibb & Colquhoun, 1992).

Modulation of NMDAR channel activity by $[Ca^{2+}]_i$ in cell-attached mode. When the recording pipette contained 5 μM NMDA, 10 μM glycine and 5 mM BAPTA (to prevent influx of Ca^{2+}), the open probability (NP_o) of the NMDAR channels calculated for records with a duration of 10 s was relatively stable and varied between 0·015 and 0·03 (Fig. 7A and Fig. 8C, cell-attached). Pressure application of NMDA to the soma of the neurone induced a rapid depolarization which resulted in the decrease of current amplitude (Fig. 7A and B). After application of the agonist the amplitude of the NMDA-activated currents recovered to the control level during 1–2 s, reflecting restoration of the resting potential. However, the activity of NMDAR channels after conditioning applications was much lower than in control (NP_o less than 0·005) and recovered to control levels during 90 s (Figs 7A and 8C). A similar effect was observed in twenty-eight out of thirty-four cell-attached patches.

This observation, similar to that reported previously (Legendre *et al.* 1993), indicates that the Ca^{2+} influx produced by a conditioning NMDA application causes inhibition of NMDAR channels by acting at the cytoplasmic side of the membrane.

During prolonged recording (from 7 to 19 min) in five cell-attached patches, repetitive (with 1·5–2 min intervals) applications of conditioning NMDA to the soma of the neurones caused reproducible decreases in NP_o, showing that Ca^{2+}-induced inactivation of single NMDAR channels did not change during this time of the recording. In two other patches, the decrease of NP_o was observed only after the first conditional application of NMDA.

On average, after conditioning NMDA applications to the soma of neurones, NP_o decreased by 72 ± 6% ($n = 5$, Fig. 7C and D). The time course of the recovery from Ca^{2+}-induced inactivation varied for different cell-attached patches from 20 to 100 s ($n = 14$, Fig. 7C). These kinetics coincide with the time course of the Ca^{2+}-dependent fluorescence recovery after conditioning NMDA applications (Fig. 2, Table 1).

Figure 7D summarizes the effect of Ca^{2+} influx on the main kinetic parameters of NMDAR channels in cell-attached configuration. Control values were taken as 1. Parameters were estimated from the first 20 s after conditioning NMDA applications. It is seen that $[Ca^{2+}]_i$ elevation cause a decrease

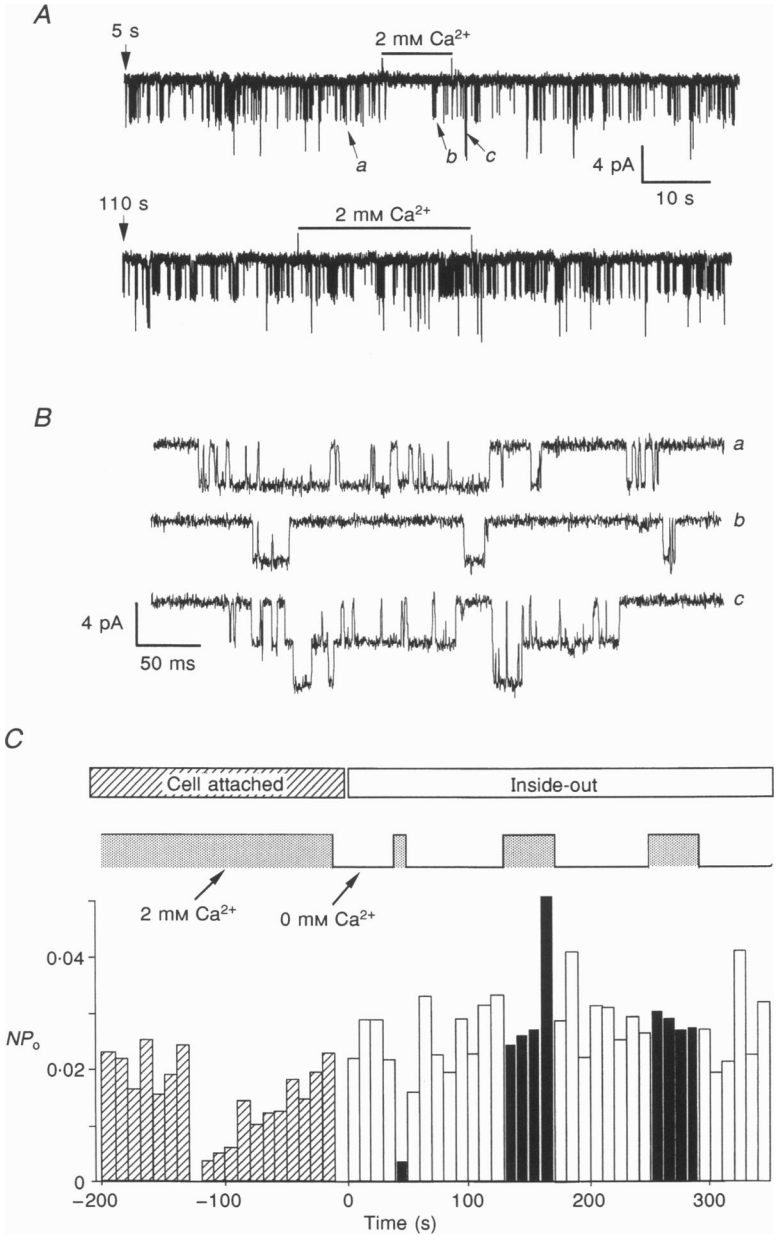

Figure 8. Ability of Ca^{2+} to inhibit NMDAR channels in inside-out patches

Membrane potential, −50 mV. Two seconds before obtaining an inside-out patch the neurone was bathed with external Ca^{2+}-free solution containing 5 mM BAPTA. During the experiment the BAPTA-containing solution was replaced a few times by an external solution containing 2 mM Ca^{2+} using a fast perfusion system. Same patch as in Fig. 7*A* and *B*. *A*, slow time base: the traces illustrate the activity of the NMDAR channels just after obtaining the inside-out patch (upper trace) and after 110 s of recording (lower trace). The durations of Ca^{2+} applications are shown by bars. For display, traces were digitized at 1 kHz. Note that the second application of Ca^{2+} (much longer than the first) was ineffective. *B*, fast time base: the traces illustrate the single NMDAR channel current activity at the time points marked in the upper trace of Fig. 8*A* by *a*, *b* and *c*. The traces were digitized at 10 kHz. Notice in trace *b* the decrease in frequency of activation with no change in current amplitude. *C*, plot of the NMDAR channel NP_o variations during cell-attached and inside-out recordings illustrated in Figs 7*A* and 8*A*. The durations of the NMDA application in cell-attached configuration and Ca^{2+} applications in inside-out configuration are shown by filled bars. Time zero corresponds to the beginning of the inside-out recording. Each column represents NP_o calculated for consecutive 10 s duration records. Before the transition to the inside-out mode, NMDAR channel activity was recorded for 6 min in the cell-attached configuration. Two successive applications of NMDA caused a strong decrease in NP_o similar to that presented in the plot of the second NMDA application in cell-attached mode. Note that only the first exposure of the inside-out patch to Ca^{2+} resulted in a decrease of the NMDAR channel activity. Subsequent applications did not modulate NP_o.

in the NP_o and in the frequency of NMDAR channel activity without pronounced effects on the open time parameters. The most sensitive parameter to the modulatory action of $[Ca^{2+}]_i$ is the slow closed time component which increased, on average, about 5-fold.

Modulation of NMDAR channel activity by $[Ca^{2+}]_i$ in inside-out mode. Figure 8 illustrates the continuation of the experiments presented in Fig. 7*A* and *B*. The activity of NMDAR channels recorded in the cell-attached mode were now analysed after obtaining inside-out patches at a membrane potential of −50 mV. In the presence of 2 mM BAPTA in the external solution the transition from cell-attached to inside-out mode was not accompanied by significant changes in NP_o (Fig. 8*C*). In the absence of Ca^{2+} on the cytoplasmic side of the membrane, the activity of NMDAR channels was stable showing mainly one level of activation with rare simultaneous activation of two channels (Fig. 8*A*). Forty seconds after obtaining the inside-out patch a fast application of Ca^{2+} to the cytoplasmic part of the membrane (2 mM, 10 s) resulted in a decrease of NP_o from 0·021 to less than 0·005 (NP_o averaged during 10 s of the recording). Ca^{2+} induced a decrease in the frequency of NMDAR channel activation without changes in the current amplitude (Fig. 8*Bc*). Washing with Ca^{2+}-free solution restored the activity of NMDAR channels to control levels (Fig. 7*A* and *C*). However, subsequent exposure to 2 mM Ca^{2+} (after 130 and 250 s of inside-out patch) failed to decrease the activity of NMDAR channels (Fig. 8*A*, lower trace, and *C*). This effect was observed in thirteen out of twenty-nine inside-out patches. In the remaining sixteen patches the modulatory action of Ca^{2+} was absent even at the first exposure.

During the first 30–60 s of inside-out recording in patches isolated from cerebellar granule cells, application of

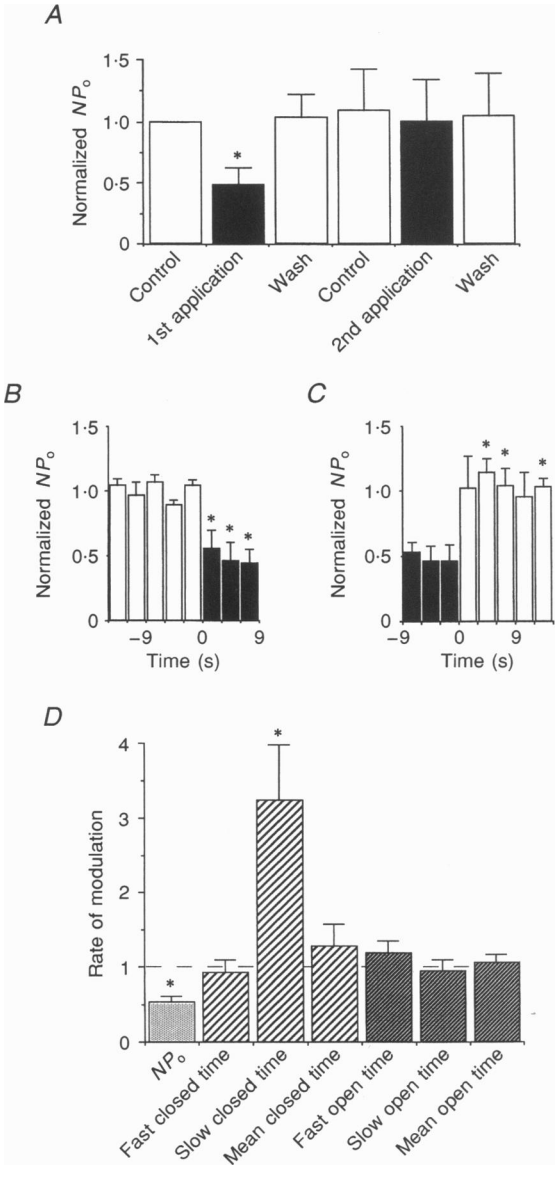

Figure 9. Summary data for Ca^{2+}-induced inactivation of the NMDAR channels in inside-out patches

The data illustrated are the means ± S.E.M. of 6 experiments. All patches were obtained in the presence of 5 mM BAPTA as described in the legend to Fig. 8 and Methods. Membrane potential, −50 mV. Statistical significance (*) was established using a Student's *t* test ($P < 0·05$). *A*, effect of Ca^{2+} on the P_o of the NMDAR channels. □, 5 mM BAPTA; ■, 2 mM Ca^{2+}. NP_o of each experiment was normalized to the mean NP_o of channels before the 1st application of Ca^{2+}. 'Control' columns represent NP_o calculated for records lasting between 20 and 50 s in different experiments. Columns labelled '1st application' and '2nd application' are the NP_o values calculated during application of 2 mM Ca^{2+} to inside-out patches from internal side of membrane (records lasting between 20 and 60 s). Columns labelled 'wash' illustrate NP_o values obtained for 20 s records after Ca^{2+} application. Note the significant decrease in the NP_o during 1st application of Ca^{2+}, and absence of the effect during the 2nd Ca^{2+} application. *B* and *C*, change in NP_o of the NMDAR channels during (*B*) and after (*C*) application of 2 mM Ca_i^{2+}. □, 5 mM BAPTA; ■, 2 mM Ca^{2+}. Time zero corresponds to the beginning of changes in $[Ca^{2+}]_i$. Each column represents NP_o calculated for consecutive 3 s duration records. NP_o in each experiment was normalized to mean NP_o of channels before application of Ca^{2+}. To determine the significance of the change in NP_o after modulation of $[Ca^{2+}]_i$ the values which correspond to columns on the right of the graphs (positive time range) were compared with mean NP_o of the NMDAR channels before changes in $[Ca^{2+}]_i$ (negative time range). Note the fast changes in NP_o following changes in $[Ca^{2+}]_i$. *D*, effect of $[Ca^{2+}]_i$ on the kinetic parameters of NMDAR channels. The columns represent the ratio between the control value (results of analysis of 20–30 s records before application of 2 mM Ca_i^{2+}) and that obtained during first application of $[Ca^{2+}]_i$. All parameters were calculated as described in the legend to Fig. 7*D*.

micromolar Ca^{2+} concentration (10 μM) resulted in a transient decrease in NP_o of 39·7 ± 6% ($n = 8$). Following 3–5 min of recording, Ca^{2+} became ineffective.

Figure 9 summarizes results obtained from this set of experiments in hippocampal patches which had a stable activity in BAPTA solution (absence of run-down). The first exposure of Ca^{2+} to the cytoplasmic side of the membrane caused a decrease in NP_o of NMDAR channels by 51 ± 11% ($n = 7$) while the second exposure was not effective (Fig. 9*A*). As in the cell-attached records, the inhibitory action of $[Ca^{2+}]_i$ on NMDAR channels resulted in an increase (more than 3-fold) in the slow closed time component without a pronounced effect on the open time parameters (Fig. 9*D*).

Detailed analysis of the kinetics of Ca^{2+}-induced modulation of NMDAR channels was limited by the loss of NMDAR channels sensitivity to Ca^{2+}. Figure 9*B* and *C* demonstrates that, on average, the transition of NP_o caused by fast application and removal of 2 mM Ca^{2+} on the cytoplasmic side of the membrane develops in less than 3 s.

Thus, these results demonstrate a fast washout of NMDAR channels sensitivity to cytoplasmic Ca^{2+} in conditions where irreversible run-down was not observed. These data also indicate that the inhibitory action of $[Ca^{2+}]_i$ on NMDAR channels is a relatively fast process.

DISCUSSION

In both rat hippocampal and cerebellar granule neurones elevation of $[Ca^{2+}]_i$ causes two main types of NMDAR channel modulation: Ca^{2+}-induced irreversible inhibition (run-down) and transient inactivation. They have some common features and specific differences. Thus, both phenomena (i) are prevented by using Ca^{2+}-free external solution or by strong buffering of the intracellular Ca^{2+} by BAPTA (Rosenmund & Westbrook, 1993*a*, *b*; Legendre *et al.* 1993; Medina *et al.* 1994) and (ii) decrease the NMDA-activated current by about 30–50% (Legendre *et al.* 1993; Vyklický, 1993; Medina *et al.* 1994, 1995).

On the other hand, run-down is an ATP-dependent process: the irreversible decrease of NMDA-activated currents can be prevented or retarded by inclusion of ATP-regenerating solutions in the recording pipette (MacDonald, Mody & Salter, 1989; Rosenmund & Westbrook, 1993*a*; present study). In contrast, ATP had no effect on the Ca^{2+}-induced transient inactivation of NMDAR channels (Vyklický, 1993; present study), which suggests that this phenomenon is not mediated by phosphorylation/dephosphorylation processes.

The main conclusion from the present study is that the transient Ca^{2+}-induced inactivation of NMDAR and the irreversible run-down develop via different mechanisms. Several lines of evidence support this conclusion: (i) in most of the granule cells, and in some of the hippocampal neurones, transient inactivation disappeared in the absence of run-down; (ii) in contrast, in hippocampal neurones under conditions of accelerated run-down (ATP-free pipette solution) the transient inactivation of NMDA-activated currents does not disappear; (iii) in inside-out patches the NMDAR channels may be reversibly inhibited by $[Ca^{2+}]_i$ but the time-dependent disappearance of the sensitivity to $[Ca^{2+}]_i$ is not associated with a decrease in NMDAR channel activity.

The relationship between $[Ca^{2+}]_i$ and Ca^{2+}-dependent inactivation of NMDAR channels

Our data indicate that during whole-cell recording the inhibitory action of $[Ca^{2+}]_i$ on NMDAR channels in cerebellar granule cells and in hippocampal neurones is proportional to $[Ca^{2+}]_i$ changes. The analysis of the degree of dependence of NMDAR test currents on the amount of conditioning charge (which is proportional to Ca^{2+} influx) revealed that the threshold of inhibition was observed at conditioning charges of 0·05–0·1 nC and reached maximum at charges of 0·3–0·4 and 0·5–0·10 nC in granule cells and hippocampal neurones, respectively (Figs 1 and 5). Elevation of external Ca^{2+} enhanced the degree of transient NMDAR channel inhibition.

Several arguments indicate that the effect of Ca^{2+} did not require its passing via NMDAR channels. Its action develops on the inner part of the membrane independently of the source of Ca^{2+}. This conclusion is based on the following observations: (i) single NMDAR channels in cell-attached or inside-out patch mode are inhibited by Ca^{2+} acting from the cytoplasmic part of the membrane (Legendre *et al.* 1993; Vyklický, 1993, present study); (ii) selective influx of Ca^{2+} via kainate-activated channels results in the inhibition of NMDAR channels (Medina *et al.* 1994; Kyrozis, Goldstein, Heath & MacDermott, 1995); (iii) co-expression of Ca^{2+}-impermeable NMDAR and Ca^{2+}-permeable AMPAR subunits in HEK293 cells showed that selective influx of Ca^{2+} via AMPA-activated channels causes inhibition of NMDAR mutants (N. Burnashev, P. Bregestovski, P. Seeburg & B. Sakmann, unpublished observations).

This raises the possibility that elevation of $[Ca^{2+}]_i$ via voltage-gated Ca^{2+} channels or from other sources can cause a modulation of NMDAR components in dendritic spines of glutamatergic synapses during excitation. Indeed, recently it was demonstrated that elevation of $[Ca^{2+}]_i$ during depolarization causes transient inhibition of NMDAR component of synaptic current (Rosenmund *et al.* 1995; Medina *et al.* 1995).

Kinetics of $[Ca^{2+}]_i$ action on NMDAR channels

Previous observations in hippocampal neurones and HEK293 cells suggested that the action of $[Ca^{2+}]_i$ on NMDAR channels is a relatively slow process. Indeed, in different studies the recovery of NMDAR channels from Ca^{2+}-induced inhibition developed in the range of 10–100 s (Legendre *et al.* 1993; Vyklický, 1993; Bregestovski, Medina & Ben-Ari, 1994; Medina *et al.* 1994). Two observations of the present study suggest that this process is much faster

and the slow time course of NMDAR channel recovery from inhibition actually reflects the kinetics of $[Ca^{2+}]_i$ transients. First, simultaneous monitoring of $[Ca^{2+}]_i$ and NMDA-activated currents revealed a close correlation between the time constants of NMDA-induced test current recovery from transient inhibition and relaxation of $[Ca^{2+}]_i$ to the basal level (Table 1). Second, application of Ca^{2+} to the cytoplasmic side of the membrane in inside-out patches provides direct evidence that the modulatory action of $[Ca^{2+}]_i$ develops in less than 3 s. Recording of single-channel activity with a few channels in the patch and fast washout of Ca^{2+}-sensitivity did not allow us to evaluate the precise kinetics of $[Ca^{2+}]_i$ action on NMDAR channels.

Recent studies on neocortical (Markram, Helm & Sakmann, 1995) and hippocampal CA1 (Jaffe, Johnston, Lasser-Ross, Lisman, Miyakava & Ross, 1992; Spruston, Schiller, Stuart & Sakmann, 1995) neurones in slices showed that dendritic $[Ca^{2+}]_i$ transients develop in a time scale from several hundred milliseconds to several seconds. Our results suggest that the modulatory action of Ca^{2+} on NMDAR channels can take place in a physiologically relevant time scale.

Transient inactivation and run-down: common or different pathways of Ca^{2+} action?

As a possible explanation of inhibitory Ca^{2+} action on NMDAR channels, Rosenmund & Westbrook (1993*b*) proposed a model which includes a regulatory Ca^{2+}-dependent intermediate protein associated with NMDAR and actin filaments. Elevation of $[Ca^{2+}]_i$ causes the transient dissociation of this protein from NMDAR, leading to the reversible inactivation of the channel. Actin depolymerization (stimulated by Ca^{2+} or lack of ATP) results in the loss of the regulatory protein and irreversible inactivation of the NMDAR channel (run-down). Thus, in this model, both phenomena (transient inactivation and run-down of NMDAR channels) should develop in a successive manner. The results of our whole-cell experiments on hippocampal neurones with ATP-free intracellular solutions do not satisfy this hypothesis. Indeed, the irreversible decrease in NMDA responses (run-down) was not associated with a change in the degree of Ca^{2+}-induced transient inactivation (Fig. 3).

Several other observations from the present study did not reveal correlation between transient inactivation and run-down. First, modulation of the run-down by phosphatase inhibitors or by ATP did not result in a change in the degree of transient inactivation. Second, in experiments with whole-cell recording, inactivation disappeared under conditions where run-down was absent. This effect was observed in some hippocampal neurones and it was particularly pronounced in granule cells which have a smaller size and thus, are more liable to intracellular dialysis (Figs 4 and 6). Third, in inside-out patches, in conditions where run-down of NMDAR channels was absent, ability of Ca^{2+} to transiently inhibit NMDAR channels disappeared following 3–5 min after excision (Figs 8 and 9*A*). These results allow us to suggest that Ca^{2+}-induced transient inactivation evolves independently from run-down.

Does Ca^{2+} modulate NMDAR channels directly or via intermediates?

Analysis of the action of Ca^{2+} on NMDAR channels in isolated patches was performed previously in two studies (Rosenmund & Westbrook, 1993*b*; Vyklický, 1993) and produced two apparently opposite conclusions.

Using inside-out patches from cultured hippocampal neurones, Rosenmund & Westbrook (1993*b*) showed that the activity of NMDAR channels was unaffected by exposure to 0·1–1 mM Ca^{2+} on the cytoplasmic side of the membrane. It was concluded that inhibition of NMDAR channels by $[Ca^{2+}]_i$ is restricted to intact cells. These authors suggested that Ca^{2+}-induced inhibition of NMDAR channels is not the result of direct binding to the channel and that the action of Ca^{2+} requires an intracellular factor which can be washed out from inside-out patches. In the other study, on the same preparation, reversible inhibition of NMDAR channels was recorded during exposure of the cytoplasmic side of the membrane to Ca^{2+} (Vyklický, 1993). As an explanation, this author suggested a direct action of Ca^{2+} on NMDAR channels, not excluding the possibility of Ca^{2+}-induced modulation via a component of the plasma membrane or a protein closely associated with the NMDAR channel. The evolution of $[Ca^{2+}]_i$ inhibitory action on NMDAR channels in inside-out patches during prolonged recordings was not, however, analysed in these studies.

Our observations resolve an apparent contradiction between previous observations. We show that during the first few (1–3) minutes of recording from inside-out patches single-channel activity of NMDAR can be reversibly inhibited by exposure to 10 μM or 2 mM Ca^{2+}. However, after 3–5 min of recording, NMDAR channels become insensitive to Ca^{2+}. For many patches, the loss of sensitivity to $[Ca^{2+}]_i$ developed without a decrease in the open probability of NMDAR channels, i.e. in the absence of run-down. This observation is confirmed also by results of the whole-cell recording when inactivation disappeared under conditions where run-down was absent.

These results strongly suggest the existence of a Ca^{2+}-dependent cytoplasmic intermediate which inactivates the NMDAR and washes out during the first minutes after obtaining excised patches. The possibility of a direct action of Ca^{2+} on NMDAR channels is still not completely excluded. One can suggest that the transition to the inside-out configuration causes a slow (3–5 min) and irreversible inactivation of a Ca^{2+}-binding site on the intracellular loop of the NMDAR channel protein.

Proposed scheme

The results described in this study support a model in which Ca^{2+}-induced transient inactivation of NMDAR channels develops through a run-down-independent pathway. The inhibitory action of Ca^{2+} can be observed only in the

presence of two components on the cytoplasmic side of the membrane: Ca^{2+} itself and the other, a putative Ca^{2+}-dependent regulatory factor. When this factor is absent the function of NMDAR channels cannot be modulated by Ca^{2+}.

In normal physiological conditions a 'Ca^{2+}-sensitive factor' is associated, or in close vicinity to the NMDAR protein. By itself this factor does not modulate activity of the NMDAR channel but an increase in $[Ca^{2+}]_i$ leads to transient inactivation. In hippocampal neurones we have observed Ca^{2+}-induced inactivation of the NMDA-activated currents in all whole-cell experiments ($n > 200$) and in most of the cell-attached patches (28 out of 34), which supports the view that in normal physiological conditions the NMDAR channel is ready to be inactivated. The washout of the regulatory factor does not change the ability of NMDAR channels to be activated by agonists. However, in the absence of the regulatory factor NMDAR channels become Ca^{2+}-insensitive. This is supported by experiments in whole-cell and inside-out configurations when the Ca^{2+} sensitivity of the NMDAR channels disappeared in the absence of run-down.

Transient inhibition of voltage-gated and receptor-operated channels by cytoplasmic Ca^{2+} seems to be a wide phenomenon. For L-type voltage-gated Ca^{2+} channels this effect was first discovered in *Paramecium* (Brehm & Eckert, 1978) and has since been reported in many different cell types, including neurones and heart myocytes (see Imredy & Yue, 1994). Inhibition of K^+ channels by intracellular Ca^{2+} was described in human T-lymphocytes (Bregestovski, Redkozubov & Alexeev, 1986) and observed recently in neurones (Selyanko & Brown, 1996). For receptor-operated channels, Ca^{2+}-induced inhibition was reported for acetylcholine-activated channels in the snail neurones (Chemeris, Kazachenko, Kislov & Kurchikov, 1984), and for $GABA_A$ receptor-activated channels in rat hippocampus (Inoue, Oomura, Yakushiji & Akaike, 1986; see Chen & Wong, 1995). Cyclic nucleotide-gated channels of olfactory receptor neurones (Kramer & Siegelbaum, 1992) and retinal rod photoreceptors (Nakatani, Koutalos & Yau, 1995) also show the effect. Finally, Ca^{2+}-mediated inactivation of NMDAR channels was observed in spinal (Mayer & Westbrook, 1985), hippocampal (Clark, Clifford & Zorumski, 1990; Legendre *et al.* 1993; Vyklický, 1993), dorsal horn (Kyrozis *et al.* 1995) and cerebellar granule (this study) neurones.

The mechanism of $[Ca^{2+}]_i$ modulatory action seems to be different for different types of channels. There are, however, a number of similarities in the modulatory action of Ca^{2+} on NMDAR channels and on the cyclic nucleotide-gated (CNG) channels. Thus, (i) Ca^{2+} acts from the inner part of the membrane; (ii) Ca^{2+} suppresses NMDAR and CNG channels even in the closed state; (iii) Ca^{2+}-dependent inhibition is not mediated by phosphorylation/dephosphorylation processes; and (iv) the ability of Ca^{2+} to inhibit NMDAR and CNG channels gradually decreases with the time of recording (washout of Ca^{2+}-dependent inhibition). Kramer & Siegembaum (1992) proposed that internal Ca^{2+} induces inhibition of CNG channels via a putative Ca^{2+}-binding protein. A similar suggestion arose from recent observations on bullfrog retinal rod photoreceptors (Nakatani *et al.* 1995).

The nature of the Ca^{2+}-sensitive regulatory factor of NMDAR channels needs to be determined. Eukaryotic cells contain a variety of Ca^{2+}-dependent proteins and several of them have been found in neurones (for review, see Heizmann & Hunziker, 1991). Expression of Ca^{2+}-binding proteins in different types of neurones is quite distinct. For instance, parvalbumin is present only in GABAergic interneurones (Rogers, 1989; Miettinen *et al.* 1992), while the granule cells of rat cerebellum do not show immunoreactivity to calbindin, calcineurin or parvalbumin (Heizmann & Hunziker, 1991). Comparative analyses in hippocampal neurones and cerebellar granule cells allow us to suggest that these Ca^{2+}-binding proteins are not involved in the process of Ca^{2+}-induced inactivation of NMDAR channels.

Ascher, P., Bregestovski, P. & Nowak, L. M. (1988). *N*-Methyl-D-aspartate-activated channels of mouse central neurones in magnesium-free solution. *Journal of Physiology* **399**, 207–226.

Ascher, P. & Nowak, L. M. (1988). The role of divalent cations in the *N*-methyl-D-aspartate responses of mouse central neurones in culture. *Journal of Physiology* **399**, 247–266.

Bregestovski, P., Medina, I. & Ben-Ari, Y. (1994). Modulation of NMDA currents in hippocampal neurones. In *Cellular Mechanisms of Sensory Processing*, ed. Urban, L., pp. 161–172. Springer-Verlag, Berlin.

Bregestovski, P., Redkozubov, A. & Alexeev, A. (1986). Elevation of intracellular calcium reduces voltage-dependent potassium conductance in human T cells. *Nature* **319**, 776–778.

Brehm, P. & Eckert, R. (1978). Calcium entry leads to inactivation of calcium channel in *Paramecium*. *Science* **202**, 1203–1206.

Chemeris, N. K., Kazachenko, V. N., Kislov, A. N. & Kurchikov, A. L. (1982). Inhibition of acetylcholine responses by intracellular calcium in *Lymnaea stagnalis* neurones. *Journal of Physiology* **323**, 1–19.

Chen, Q. X. & Wong, R. K. S. (1995). Suppression of $GABA_A$ receptor responses by NMDA application in hippocampal neurones acutely isolated from the adult guinea-pig. *Journal of Physiology* **482**, 353–362.

Clark, G. D., Clifford, D. B. & Zorumski, C. F. (1990). The effect of agonist concentration, membrane voltage and calcium on *N*-methyl-D-aspartate receptor desensitization. *Neuroscience* **39**, 787–797.

Gibb, A. & Colquhoun, D. (1992). Activation of *N*-methyl-D-aspartate receptors by L-glutamate in cells dissociated from adult rat hippocampus. *Journal of Physiology* **456**, 143–179.

Heizmann, C. & Hunziker, W. (1991). Intracellular calcium-binding proteins: more sites than insights. *Trends in Biological Sciences* **16**, 91–103.

Hollmann, M. & Heinemann, S. (1994). Cloned glutamate receptors. *Annual Review of Neuroscience* **17**, 31–108.

Imredy, J. P. & Yue, D. P. (1994). Mechanism of Ca^{2+}-sensitive inactivation of L-type Ca^{2+} channels. *Neuron* **12**, 1301–1318.

INOUE, M., OOMURA, Y., YAKUSIJI, T. & AKAIKE, N. (1986). Intracellular calcium ions decrease the affinity of the GABA receptor. *Nature* **234**, 156–158.

JAFFE, D. B., JOHNSTON, D., LASSER-ROSS, N., LISMAN, J. E., MIYAKAWA, H. & ROSS, W. N. (1992). The spread of Na^+ spikes determines the pattern of dendritic Ca^{2+} entry into hippocampal neurons. *Nature* **357**, 244–246.

KRAMER, R. H. & SIEGELBAUM, S. A. (1992). Intracellular Ca^{2+} regulates the sensitivity of cyclic nucleotide-gated channels in olfactory receptor neurons. *Neuron* **9**, 897–906.

KYROZIS, A., GOLDSTEIN, P., HEATH, M. & MACDERMOTT, A. (1995). Calcium entry through a subpopulation of AMPA receptors desensitized neighbouring NMDA receptors in rat dorsal horn neurons. *Journal of Physiology* **485**, 373–381.

LEGENDRE, P., ROSENMUND, C. & WESTBROOK, G. L. (1993). Inactivation of NMDA channels in cultured hippocampal neurons by intracellular calcium. *Journal of Neuroscience* **13**, 674–684.

MACDONALD, J., MODY, I. & SALTER, M. (1989). Regulation of *N*-methyl-D-aspartate receptors revealed by intracellular dialysis of murine neurones in culture. *Journal of Physiology* **414**, 17–34.

MARKRAM, H., HELM, P. J. & SAKMANN, B. (1995). Dendritic calcium transients evoked by single back-propagating action potentials in rat neocortical pyramidal neurons. *Journal of Physiology* **485**, 1–20.

MAYER, M., VYKLICKÝ, L. & CLEMENTS, J. (1989). Regulation of NMDA receptor desensitization in mouse hippocampal neurons by glycine. *Nature* **338**, 425–427.

MAYER, M. L. & WESTBROOK, G. L. (1985). The action of *N*-methyl-D-aspartic acid on mouse spinal neurones in culture. *Journal of Physiology* **361**, 65–90.

MAYER, M. L. & WESTBROOK, G. L. (1987). The physiology of excitatory amino acids in the vertebrate central nervous system. *Progress in Neurobiology* **28**, 197–276.

MEDINA, I., BREGESTOVSKI, P. & BEN-ARI, Y. (1993). Recovery from desensitization of NMDA-activated currents in cultured hippocampal neurones is modulated by intracellular calcium. *Journal of Neurochemistry* **61**, S257.

MEDINA, I., FILIPPOVA, N., BARBIN, G., BEN-ARI, Y. & BREGESTOVSKI, P. (1994). Kainate-induced inactivation of NMDA currents via an elevation of intracellular Ca^{2+} in hippocampal neurons. *Journal of Neurophysiology* **72**, 456–465.

MEDINA, I., FILIPPOVA, N., CHARTRON, G., ROUGEOLE, S., BEN-ARI, Y., KHRESTCHATISKY, M. & BREGESTOVSKI, P. (1995). Calcium-dependent inactivation of heteromeric NMDA receptor–channels expressed in human embryonic kidney cells. *Journal of Physiology* **482**, 567–573.

MEDINA, I., LEINENKUGEL, X., ROVIRA, C., BEN-ARI, Y. & BREGESTOVSKI, P. (1995). Double patch-clamp analysis of Ca^{2+}-inactivation of NMDA synaptic currents. *Society for Neuroscience Abstracts* **21**, 244.17.

MIETTINEN, R., GULYAS, A., BAIMBRIDGE, K., JACOBOWITZ, D. & FREUND, T. (1992). Calretinin is present in non-pyramidal cells of the hippocampus – II. Co-existence with other calcium binding proteins and GABA. *Neuroscience* **48**, 29–43.

NAKATANI, K., KOUTALOS, Y. & YAU, K.-W. (1995). Ca^{2+} modulation of the cGMP-gated channel of bullfrog retinal rod photoreceptors. *Journal of Physiology* **484**, 69–76.

NOWAK, L., BREGESTOVSKI, P., ASCHER, P., HERBET, A. & PROCHIANTZ, A. (1984). Magnesium gates glutamate-activated channels in mouse central neurones. *Nature* **307**, 462–465.

ROGERS, J. (1989). Immunoreactivity for calretinin and other calcium-binding proteins in cerebellum. *Neuroscience* **31**, 711–721.

ROSENMUND, C., FELTZ, A. & WESTBROOK, G. (1995). Calcium-dependent inactivation of synaptic NMDA receptors in hippocampal neurons. *Journal of Neurophysiology* **73**, 427–430.

ROSENMUND, C. & WESTBROOK, G. L. (1993*a*). Run-down of *N*-methyl-D-aspartate channels during whole-cell recording in rat hippocampal neurons: Role of Ca^{2+} and ATP. *Journal of Physiology* **470**, 705–729.

ROSENMUND, C. & WESTBROOK, G. L. (1993*b*). Calcium-induced actin depolymerization reduces NMDA channel activity. *Neuron* **10**, 805–814.

SATHER, W., DIEUDONNE, S., MACDONALD, J. F. & ASCHER, P. (1992). Activation and desensitization of *N*-methyl-D-aspartate receptors in nucleated outside-out patches from mouse neurones. *Journal of Physiology* **450**, 643–672.

SELYANKO, A. A. & BROWN, D. A. (1996). Intracellular calcium directly inhibits potassium M channels in excised membrane patches from rat sympathetic neurons. *Neuron* **16**, 151–162.

SPRUSTON, N., SCHILLER, Y., STUART, G. & SAKMANN, B. (1995). Activity-dependent action potential invasion and calcium influx into hippocampal CA1 dendrites. *Science* **268**, 297–300.

TONG, G. & JAHR, C. E. (1994). Regulation of glycine-insensitive desensitization of the NMDA receptor in outside-out patches. *Journal of Neurophysiology* **72**, 754–761.

VYKLICKÝ, L. JR (1993). Calcium-mediated modulation of *N*-methyl-D-aspartate (NMDA) responses in cultured rat hippocampal neurones. *Journal of Physiology* **470**, 575–600.

ZORUMSKI, C. F., YANG, J. & FISCHBACH, G. D. (1989). Calcium-dependent, slow desensitization distinguishes different types of glutamate receptors. *Cellular and Molecular Neurobiology* **9**, 95–104.

ZUKIN, R. S. & BENNETT, M. V. L. (1995). Alternativaly spliced isoforms of the NMDAR1 receptor subunit. *Trends in Neuroscience*, **18**, 306–312.

Acknowledgements

We wish to thank Drs Philippe Ascher and Spencer Shorte for their critical reading of the manuscript. We also would like to acknowledge Dr Evelyne Tremblay for helpful discussions concerning the preparation of cerebellar granule cell cultures and Lucyna Surzyn for technical assistance. This work was supported by grant 93-3269 from the International Association for the Promotion of Cooperation with Scientists from the Independent States of the Former Soviet Union (INTAS) and by EEC grant ERBCHBGCT930392

Authors' present addresses

N. Filippova: Institute of Developmental Biology, Russian Academy of Sciences, 26 Vavilov Street, 117334 Moscow, Russia.

A. Bakhramov: University of Oxford, Department of Pharmacology, Mansfield Road, Oxford OX1 3QT, UK.

Received 5 January 1996; accepted 15 May 1996.